Full Scale Test on a 100km, 150kV AC Cable

Faria da Silva, Filipe Farria; Wiechowski, W. ; Bak, Claus Leth; Gudmundsdottir, Unnur Stella

Published in:
Proceedings of the CIGRE Session 2010

Publication date:
2010

Document Version
Publisher's PDF, also known as Version of record

21, rue d'Artois, F-75008 PARIS
http : //www.cigre.org

B1-301

CIGRE 2010

Full Scale Test on a 100km, 150kV AC Cable

F. FARIA DA SILVA, W. WIECHOWSKI, C. LETH BAK, U. STELLA GUDMUNDSDOTTIR
Aalborg University; Energinet.dk
Denmark

SUMMARY

This paper presents some of the results obtained from the electrical measurements on a 99.7 km, 150 kV three-phase AC cable, connecting 215 MW offshore wind farm Horns Rev 2, located in Denmark west coast, to Denmark's 400 kV transmission network.
The measurements were performed at nominal voltage. The cable was energised from the grid side with the receiving end open. An 80 Mvar shunt reactor was installed in the middle of the cable and it was energised together with the cable.
The use of nominal voltage allows to present and to verify some of the phenomena that are common in long HVAC cables, but unusual in overhead lines.
In this paper is made a characterization of the cable and the power transmission system in which the cable is installed, followed by a description of the measurement equipment and of the test setup/procedures.
A theoretical explanation and presentation of different analysed phenomena is conducted. The cases analysed in this paper are: Zero-missing phenomenon, Ferranti effect, energisation transient, effect of the cable's connection in the busbar voltage and cable disconnection.
For all the phenomena described in the paper measurement data are presented and it is verified if the obtained results are in accordance with the theory and also with simulations performed in PSCAD/EMTDC.
With the exception of the cable disconnection, for all the remaining cases introduced in this paper the measurements confirmed the theoretical expectations. Depending on the cable disconnection sequence, an overvoltage may appear in one of the phases, this overvoltage depends on the mutual inductance between the shunt reactor phases and it is not shown in the simulations.
The measurement's data files and extra information about the cable and power transmission system can be received by contacting the first author of this paper.

KEYWORDS

High Voltage - Measurement - Cable - Alternating Current - Reactor - Switching - Transient - Steady State

fms@energinet.dk

INTRODUCTION

In recent years, the use of Underground Cables instead of Overhead Lines (OHL) for the transmission of electricity at high-voltage levels has become more and more common.
On the 4th of November 2008, Denmark Government decided that in order to reduce the visual pollution caused by OHL, all the transmission lines with a voltage level equal and below 150 kV must be undergrounded gradually within the next 20 years. Additionally all new 400 kV lines will be built as cable lines (with some exceptions) [1][2]. This massive use of HV cables will force to some changes in the philosophies used until now for the planning, analysis and operation of electrical power systems.
Transients measurements performed on long HV cables are uncommon, so due to this unique opportunity of having full access to a 99.7 km, 150 kV cable just before its commissioning, a group of tests for the verification of some of the phenomena characteristic for long HVAC cables and the assessment of the accuracy of the simulation models were performed.

SYSTEM CHARACTERIZATION

The Danish TSO (Energinet.dk) finished in 2009 the installation of a 99.7 km, 150 kV AC cable connection between the offshore wind farm Horns Rev 2 and the 400 kV grid, whose single-line diagram is shown in Figure 1, where points A,B and C are the measurement points.
The 99.7 km cable is divided in three parts, each consisting in three 150 kV single-core XLPE cables:

- 42 km of sea cable
- 2.3 km of land cable
- 55.4 km of land cable

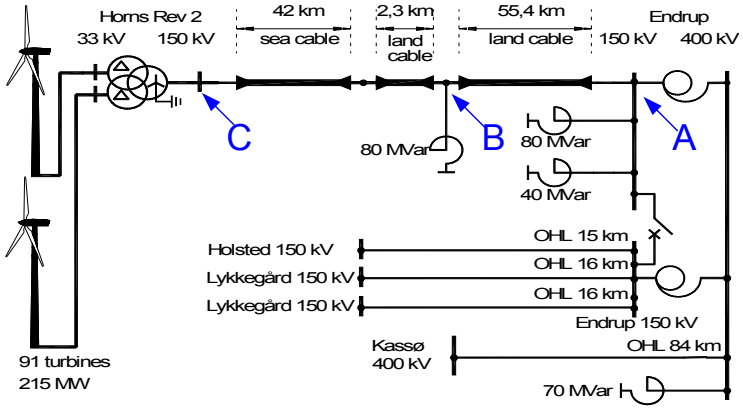

Figure 1 - Single-line diagram of the connection between Horns Rev 2 and the shore [3]

Information about the cable used in the connection of Horns Rev 2 wind farm to the shore is presented in Table 1. The land cables consist of three single-phase cables connected in flat formation, for the sea cable a common armour is used for the three conductors. The land cables' sheaths are cross-bonded and the sea cable's sheaths are bonded in both ends.
The cables' self and mutual resistance, inductance and capacitance can be consulted in Table 2 and Table 3. These parameters were corrected to include the influence of cables' semiconductive layer, and adjusted capacitance and resistance, as according to [4].
In order to compensate the reactive power generated by the cable, an 80 Mvar three-phase-five legs shunt reactor was installed in the middle of the cable line (see Figure 1). Other two shunt reactors of 80 Mvar and 40 Mvar were installed onshore, in the 150 kV side of the substation (see Figure 1).

Table 1 - Basic information on Horns Rev 2 cable

	Length [km]	Conductor material	Cross-section [mm^2]	Insulation Thickness [mm]	Sheath Thickness [mm]	Cable Diameter [mm]	No. Segments	Average Segment length [km]
Sea Cable	42	Copper	630	18	2.4	208*	1	42
Long Land Cable	55.4	Aluminium	1200	17	1.289	95	33	1.8**
Short Land Cable	2.3	Aluminium	1200	17	1.289	95	4	***

* In the sea cable the same armour is common to the three conductors

** Some segments are shorter

*** The segments have all different lengths (951.5 m, 38.6 m, 728.7 m and 742.3 m)

Table 2 - Cables' self Resistance, Inductance and Capacitance

	Conductor Resistance [Ω/km]	Conductor Reactance [Ω/km]	Sheath Resistance [Ω/km]	Sheath Reactance [Ω/km]	Conductor-Sheath Capacitance [μF/km]	Sheath-Armour Capacitance [μF /km]
Land Cables	$75.35x10^{-3}$	0.688	0.157	0.629	0.223	1.783
Sea Cables	$78.66x10^{-3}$	0.708	0.424	0.533	0.175	$0.999x10^{3}$

Table 3 - Cables' mutual impedance*

	Conductor-Sheath [Ω/km]	Conductor-Conductor [Ω/km]
Land Cables	$49.27x10^{-3}$+0.630j	$49.22x10^{-3}$+0.579j
Sea Cables	$49.27x10^{-3}$+0.634j	$49.22x10^{-3}$+0.585j

*The mutual impedance between conductor-conductor and conductor-sheath of different phases is the same

TEST SETUP

Measurements were effectuated on three different points along the cable. The points and measured signals were located as follows:

- Onshore substation (Point A in Figure 1)
  - Three-phase voltages in the cable
  - Three-phase voltages in the busbar (before the circuit breaker)
  - Three-phase currents in the cable
  - Current in the surge arrester for one of the phases (not always measured)
- Shunt reactor (Point B in Figure 1)
  - Three-phase currents in the shunt reactor
- Wind Farm (Point C in Figure 1)
  - Three-phase voltages in the cable

The closing of the circuit breaker was made by synchronised switching at zero voltage. The voltage and current were reduced to values readable by the measurement equipment by using respectively inductive voltage transformers and current transformers.

The shunt reactor installed in the middle of the cable (see Figure 1) is connected directly to the cable. The two shunt reactors installed in the substation onshore were always connected several minutes before of the cable energisation, being both in steady-state during the cable energisation.To be sure that the inductive voltage transformer would not distort the measured signals, the voltage transformer

onshore (i.e. in the sending end) was tested prior to the full-scale measurements. As can be seen in Figure 2 the transformer's transfer characteristic is close to the ideal up to 1 kHz.
The cable was energised from the grid side, being the receiving end opened in the high voltage side of the wind farm's transformer. The short circuit power in the sending end remained constant during the measurements, equal to $S_k = 2372 \angle 87.91\,\text{MVA}$ on the 150 kV side of the substation.
The data in the three measurement points were acquired using an Omicron CMC 256-6 with EnerLyzer option, but while the voltage was measured directly from the inductive voltage transformers without the use of probes, for the current measurements current probes were used. Information about the Omicron technical data can be found in [5].
Steady-state measurements were always performed at a sampling frequency of 28 kHz, for the disconnections the data was acquired using a 9 kHz sampling frequency, for the connections the acquisition was made using both frequencies.
To be sure that the results were accurate the cable was energised and de-energised three times, all these transients were measured. Four steady-state measurements were also performed.

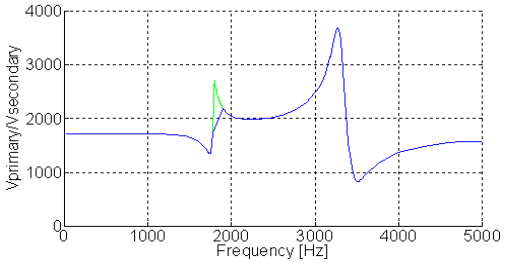

Figure 2 - Inductive voltage transformer transfer characteristic (at green fitting for the first resonance point)

SIMULATION SETUP

To simulate the system it was used PSCAD/EMTDC. The influences of the cable semiconductive layers were considered by changing the insulation permittivity [4]. The conductor and screen resistances were corrected to consider respectively the 81 segments of the conductor and the number of copper wires in screen plus the empty space between the wires. The screen thickness was also corrected to consider the empty space between the wires.
For the cross-bondings was considered a ground resistance of 3 Ω and a wire inductance of 1 μF. All the minor sections of the cross-bondings were modelled.
The shunt reactors parameters were obtained directly from the respective test reports.
To simulate the connection between the offshore wind farm and the grid two setups were designed. A first one modelling only the 150 kV grid, and not considering the shunt reactors installed in the onshore substation. A second setup with the two shunt reactors installed in the substation and the 400/150 kV transformer was also designed.
In the simulations presented in this paper is used the first setup. It will be shown in a future paper that the first setup can be used without loss of precision. For the disconnection, the setup was simplified to consider just the major sections of the cross-bonding, being also increased the fitting errors of the admittance and propagation functions. These simplifications were necessary because of passivity violations in the software's cable fitting, which would lead to an unstable simulation.

ZERO-MISSING PHENOMENON

When energizing a shunt reactor there will be both AC and DC current components. The decaying of the DC current component depends on the cable and shunt reactor resistances, and it can take several seconds to fully damp this DC current. The initial value of the DC component depends of the voltage value at the shunt reactor's terminals in the moment it is connected. If the connection is made at zero voltage the DC current is maximum, if made at a peak voltage the DC current is minimum [6].
The energisation of Horns Rev 2 cable is made using synchronised switching. As the three phases are connected for zero voltage, the initial DC component, in the shunt reactor installed in the middle of the cable, is close to the maximum.

The currents in all the three-phases of the shunt reactor in the moments after its energisation are presented in Figure 3. As previously explained the value of the DC component is maximum being its initial amplitude of approximately 400 A, a value practically equal to the amplitude of the AC component. This DC component can also be observed in the currents in the sending end as can be verified in Figure 4. Not considering the fast transients in the first milliseconds after the cable connection, which will be explained in another section, it is verified that the DC components on the cable's energised end have the same value to the ones obtained in the shunt reactor.

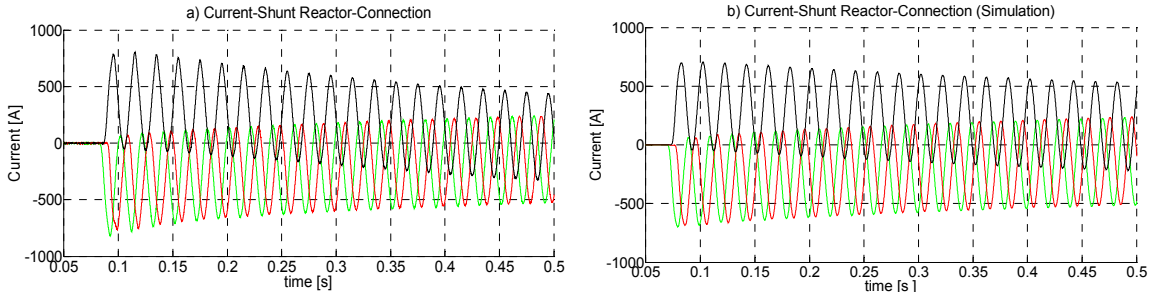

Figure 3 - Current in the three-phases of the shunt reactor in first 0.5s after the connection; a) Measured b) Simulated

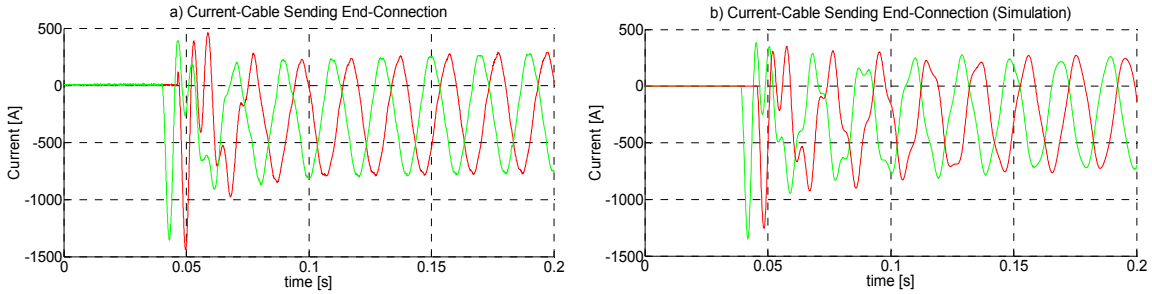

Figure 4 - Three-phases currents in the sending end in the first 0.2s after the connection; a) Measured; b) Simulated

Comparing the measurements with the simulations two important results are immediately noticed:

- The DC component is damped faster in the real system than in the simulated one;
- For the sending end, the current peak values are slightly smaller in the simulation;

If the shunt reactor was connected to an ideal voltage source, the decaying time constant would be imposed only by its inductance and resistance, 1.15H and 0.43Ω respectively, and it would be 2.67 s. But in reality the time constant is approximately 0.28 s a value 10 times smaller.
For a DC current a capacitor is an open circuit, thus the only path available for the DC current to flow is the one indicated by the dashed line in Figure 5. Thus the DC component is also damped by the cable and equivalent grid resistances, respectively 3.165 Ω and 0.4604 Ω. Therefore the time constant is not 2.67 s but the one calculated in (1).

$$\tau = \frac{1.15}{0.43 + 3.165 + 0.4604} = 0.28s \tag{1}$$

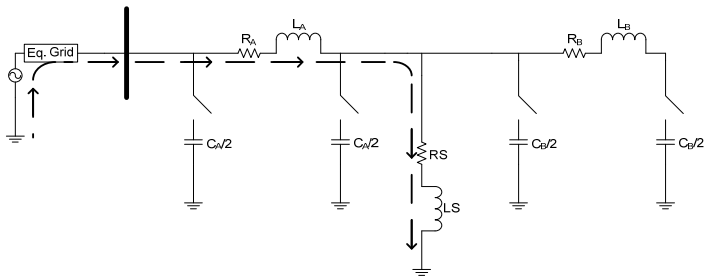

Figure 5 - Circuit seen by the shunt reactor DC current during the energisation, where: C_A and C_B are respectively the land and sea cable capacitances, R_A and R_B the land and sea cable resistances, L_A and L_B the land and sea cable inductances, RS and LS are the shunt reactor resistance and inductance

ENERGIZATION TRANSIENT

The energisation of a cable can originate a transitory overvoltage, whose peak value depends on the moment in which the cable is connected. If the circuit breaker is closed when the voltage at its terminals is zero the overvoltage is minimum, ideally zero, but if the connection is made for a peak voltage, the overvoltage is maximum. This happens due to the charging of the cable's capacitance and the energy oscillation between the cable's capacitance and inductance [7].
The energisation of Horns Rev 2 cable is made using a circuit breaker operating in synchronised switching, therefore the overvoltage and voltage distortion should be very small. That is confirmed in Figure 6, where is presented the voltage in the cable's sending end. The currents in the sending end for two of the phases, were presented in Figure 4.
As can be noticed in Figure 6 there is in the sending end a small voltage harmonic distortion and an overvoltage of almost 1.2 pu. From Figure 4 it is noticed that the current is more distorted than the voltage, and that during the first 50 ms there is a high-frequency component that is superimposed to the 50 Hz component, increasing the current amplitude. Notice that the DC component in the current is due to the shunt reactor installed in the middle of the cable, which is energised at the same time than cable. Like before the peak values are slightly smaller in the simulation than in the measurements.

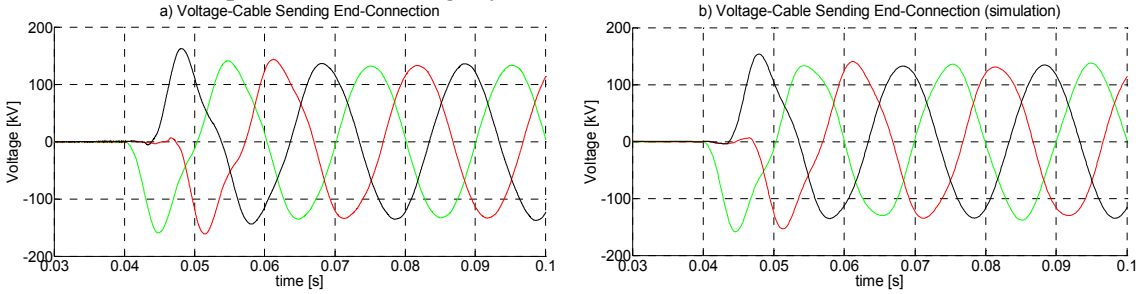

Figure 6 - Voltage in the cable's sending end during its energisation; a) Measured; b) Simulated

FERRANTI EFFECT

When a cable is unloaded or has a low load, there is a raise of the voltage in the receiving end, which becomes larger than the voltage in the sending end. For an open cable/OHL the relation between the two voltages, not considering the cable/OHL resistance, is given by (2). This phenomenon goes by the name of Ferranti Effect [8].

$$V_2 = \frac{V_1}{1 - \frac{\omega^2 LCl^2}{2}} \tag{2}$$

Where: V_1 is the voltage in the sending end; V_2 is the voltage in the receiving end; ω is the voltage frequency; L is the cable's inductance; C is the cable's capacitance; l is the cable length

From (2) it is concluded that the voltage raise is mostly dependent on the cable length. Horns Rev 2 cable is 99.7 km long and it was unloaded during the measurements, thus Ferranti Effect is expected. In Figure 7 are shown the voltages in the sending and receiving end for one of the cable's phases.

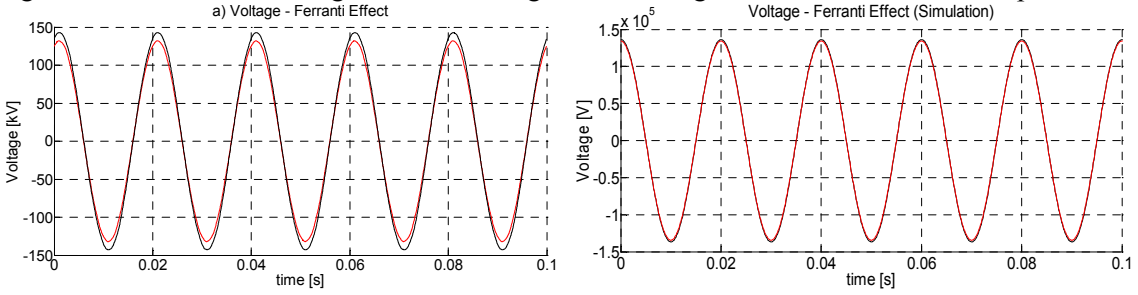

Figure 7 - Voltage in the sending end (red line) and receiving end (black line) in steady state: a) Measured; b) Simulated

For the measurements the voltage in the sending end is 162 kV while in the receiving end it is 175 kV, an 8% increase. This value was obtained with an 80 Mvar shunt reactor installed in the middle of the cable, which reduces the voltage amplitude in the receiving end, without it the voltage raise would be even larger.
In the simulation the RMS values are smaller than the measured one, being the voltage in the sending end 164.4 kV and 167.2 kV in the receiving end. While for the sending end the error is small (1.5%) for the receiving end the error is 4.7%. Also in the simulation there is almost no Ferranti Effect, the voltage raise is only of 1.7%, while in reality the voltage increased 8%.
As there was a so big difference between the measurements and the simulations, to verify if there was an error in the model, the authors designed both a new more simplify setup still using frequency-dependent model and a lumped parameters model (pi-model). Using these setups the maximum voltage raise was still only of 3%.
Due to some restrictions it was not possible to test the voltage transformer in the receiving end, but in steady-state conditions it is not expected a so large error of the measurement equipment. The authors are analyzing this difference and will present their conclusions in a future paper.

EFFECT OF THE CABLE IN THE GRID

The voltage in the cable's sending end was measured in both sides of the circuit breaker, allowing analysing how the energisation of the cable affects the grid voltage. The cable is opened in the receiving end and it is mainly capacitive, thus an increase of the voltage in the busbar is expected.
In Figure 8 are shown the voltages in the busbar during the cable's energisation. It can be noticed in the first cycle after the circuit breaker closing an increase of the voltage larger than in posterior cycles. The explanation of this behaviour was already made for the cable's energisation. It can also be verified that there is a permanent increase of the voltage in the busbar of approximately 6%. In the simulation the increase of the voltage is smaller, approximately 4.6%.

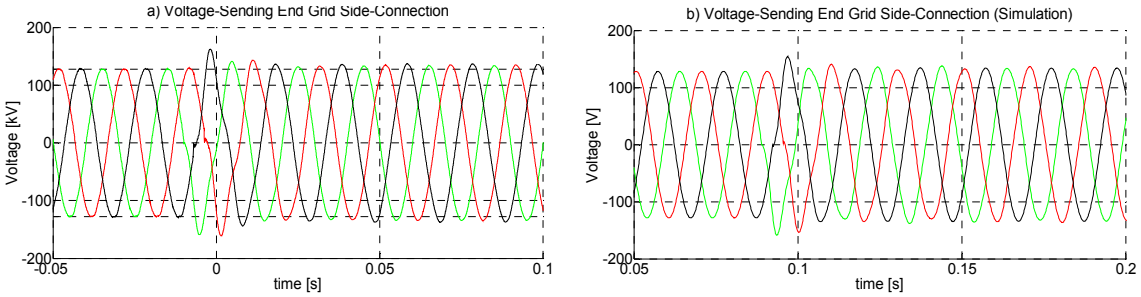

Figure 8 - Voltage in the busbar onshore during the cable's energisation: a) Measured; b) Simulated

CABLE DISCONNECTION

When a cable is disconnected the energy stored in the cable has to be damped, what due to the low cable resistance can take several seconds. As there is a shunt reactor connected directly to the cable, the stored energy will oscillate between the cable and the shunt reactor, with a resonance frequency that can be approximately calculated by (3), where L_{sh} is the shunt reactor inductance and C_{cable} is the cable capacitance. This equation does not consider the cable's inductance, which is small when compared with the shunt reactor inductance.

$$f_r = \frac{1}{2\pi\sqrt{L_{sh}C_{cable}}} \tag{3}$$

From (3) is expected a resonance frequency of approximately 33.1 Hz, the measured resonance frequency was 32.4 Hz.
But while the measured resonance frequency value is close to the expected one, the same does not apply to the voltage and current amplitudes, which show an unexpected behaviour.
Because the shunt reactor and the cable have mutual inductance between the phases and the three phases are not disconnected in the exact same moment, an overvoltage may be expected in the moments after the cable disconnection, as explained in [9] and observed in some of the simulations

(Figure 9.b). But the measurement results are different for the simulated ones, as can be observed in Figure 9 and Figure 10, which show the voltages in the cable sending end during its disconnection for both measurements and simulations.
In Figure 9.a can be observed an overvoltage in the first phase to be disconnected (red curve) and a fast damping in the last phase to be disconnected (black curve). This behaviour is not observed in the simulation (see Figure 9.b), not only the overvoltage has a smaller peak value and a longer duration it also happens for the second phase to be disconnected (green curve) and not for the first one. The fast damping of one of the phases in the first milliseconds is also not observed in the simulation (the black curve has a constant damping).
The overvoltage in the first phase to be disconnected and the fast damping in last phase to be disconnected were registered in the first and third disconnection, but not in the second one (see Figure 10.a). This is also observed in the simulations, where no overvoltage was registered for the second disconnection (see Figure 10.b). But again there are differences between the simulation and the measurement, as one of the phases is more damped in the simulation that in the measurement.
In the third disconnection, the behaviour is similar to the first disconnection.

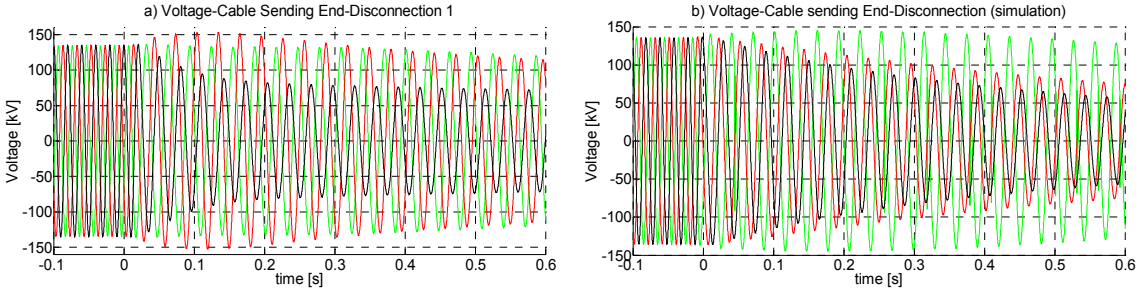

Figure 9 - Voltage in the cable sending end during the cable 1st disconnection; a) Measured;b) Simulated

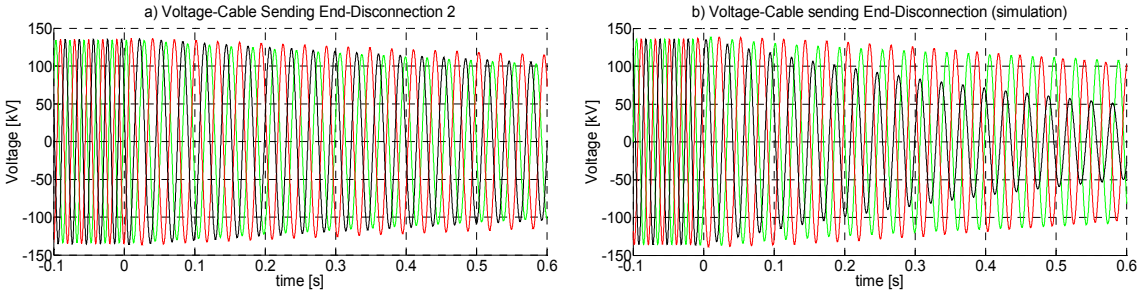

Figure 10 - Voltage in the cable sending end during the cable 2nd disconnection; a) Measured; b) Simulated

The simulations were very accurate for energisation transient, so it would also be expected accuracy for the de-energisation, but that does not happen. There are several possibilities for these differences. Due to limitations in the simulation software, the shunt reactor's mutual inductance has to be symmetrical, i.e. the mutual inductance between phases A and B has to be equal to the mutual inductance between phases B and A, in reality this does not happen.
Another possible reason for the difference may be the fact that the measurement transformers are not considered in the simulation. These transformers have inductance what may affect the disconnection transient.
More important than the differences between the measurements and the simulations, is the measured overvoltage in the first phase to be disconnected and the fast damp in the last phase to be disconnected. This behaviour is somehow unexpected, and it may be due to several reasons.
The authors noticed, by the use of simulations, that the fact of the mutual inductances do not be all equal has a strong influence in the disconnection transient, and is one of the reasons for the overvoltage. Another possible reason may be the opening of the circuit breaker not to be immediate. The circuit breaker opening time may be slightly different between phases, what influences the disconnection transient.

CONCLUSION

This paper presented results obtained in the measurement of a 99.7 km cable. The different phenomena analysed in this paper showed that transients in an HV long cable are different of transients in an OHL. Main characteristics of these transients, when using synchronised switching, are the appearing of DC currents during the connection (if shunt reactors are connected to the cable), and the long time necessary to damp the energy stored in the cable after its disconnection.
An increase of 8% of the voltage in the cable's receiving end due to Ferranti Effect was measured. The voltage raise is reduced due to the shunt reactor installed in the middle of the cable connection, without it the voltage in the receiving end would be even larger.
The more interesting results were obtained during the cable disconnection. In two of the three disconnections it was measured in the first milliseconds after the disconnection, an overvoltage in the first phase to be disconnected and a fast damping in the last phase to be disconnected. This behaviour is not shown in the performed simulations. The authors are preparing a paper explaining this phenomenon.
Some differences were register between the measurements and simulations. For the energisation transient the simulations are very accurate, being the error very small, but the same does not happen for the disconnection transient and more surprisingly neither in steady-state. For the disconnection were before presented several reasons for this difference, but no justification was found for steady-state, this situation will be deeply studied in a future paper.

FUTURE WORK

An analysis of the cable's disconnection explaining the measurement results and also the differences between the measurements and simulations is being performed.
A paper explaining the difference between the measured and simulated results for all the phenomena is also being prepared. In this paper it will also be analysed how much detail level is necessary (i.e. how many simplifications can be made) for each phenomenon under study, when modelling the cable.

BIBLIOGRAPHY

[1] Energinet.dk, "Kabelhandlingsplan 132-150kV", 2009 (in Danish)
[2] ELINFRASTRUKTURUDVALGET, "Technical Report on the future expansion and undergrounding of the electricity transmission grid", 2008
[3] W. Wiechowski, P. Børre Eriksen, "Selected Studies on Offshore Wind Farm Cable Connections - Challenges and Experience of the Danish TSO", IEEE PES GM - Conversion and Delivery of Electrical Energy in the 21st Century, 2008
[4] B. Gustavsen, J. A. Martinez, D. Durbak, "Parameter Determination for Modeling System Transients - Part II: Insulated Cables", IEEE Transactions on Power Delivery, Vol. 20, No. 3, July 2005
[5] OMICRON, "CMC 256 Hardware - Reference Manual"
[6] F. Faria da Silva, C. L. Bak, U. S. Gudmundsdottir, W. Wiechowski, M. R. Knardrupgard, "Use of a pre-insertion resistor to minimize zero-missing phenomenon and switching overvoltages", IEEE-PES General Meeting 2009
[7] Alan Greenwood, "Electric Transients in Power Systems", John Wiley & Sons, 1st Edition, 1978
[8] A. I. Ibrahim, H. W. Dommel, "A Knowledge Base for Switching Surge Transients", IPST 2005
[9] Claus L. Bak, Wojciech Wiechowski, Kim Søgaard, Søren D. Mikkelsen, "Analysis and simulation of switching surge generation when disconnecting a combined 400kV cable/overhead line with shunt reactor", IPST 2001